Nuclear Instruments and Methods in Physics Research A246 (1986) 99–104
North-Holland, Amsterdam

SUPERCONDUCTING "SNAKE" FOR THE DEDICATED SR SOURCE SIBERIA-1

V.V. ANASHIN, P.D. VOBLYI, E.S. GLUSKIN, N.I. ZUBKOV, P.M. IVANOV, P.P. ILYINSKY, V.N. KORCHUGANOV, G.N. KULIPANOV, N.A. MEZENTSEV, S.P. PETROV, A.N. SKRINSKY, A.S. SOKOLOV, E.M. TRAKHTENBERG and V.A. USHAKOV

Institute of Nuclear Physics, 630090 Novosibirsk, USSR

The storage ring Siberia-1 was put into operation as a dedicated source of synchrotron radiation at the Kurchatov Institute (Moscow) in 1983. It was designed and built at the Institute of Nuclear Physics (Novosibirsk) [1].

The critical wavelength of the radiation from the bending magnets with an electron beam in the Siberia-1 of $E = 450$ MeV is $\lambda_c = 61$ Å. This radiation has been used for experiments since 1985. In May 1985 the radiation with $\lambda_c = 21$ Å was obtained from a three-pole superconducting snake. The maximum field on the beam orbit is 4.3 T.

In the present paper the design of the snake magnet and its arrangement in the storage ring are presented as well as the results of the stand test and of the study concerning the influence of the snake on the particle motion in the storage rings.

1. Brief description of the storage ring Siberia-1, and the arrangement of the "snake" on the Siberia-1

The magnetic lattice of Siberia-1 consists of two cells comprising two C-shaped bending magnets and two straight sections. In the centre of one of the straight sections of each cell there is a quadrupole. The circumference of the magnetic lattice is 868.32 cm. The bending magnet has a maximum field of 1.5 T, a field index of 0.5 and bends the electron beam by 90°, the associated bending radius being 1 m. The length of the straight section is $l = 0.6$ m. The betatron numbers were chosen to be equal to $\nu_x = 0.793$ and $\nu_z = 0.895$ (without the "snake"). Fig. 1 shows the betatron functions $\beta_x(s)$ and $\beta_z(s)$ and also the dispersion function $\eta(s)$.

The parameters of the storage ring are listed in table 1. Fig. 2 demonstrates the arrangement of the storage ring. In the straight section 1 there is a septum magnet, RF cavity and a beam monitor. To correct the lattice chromaticities there are two sextupoles in the straight

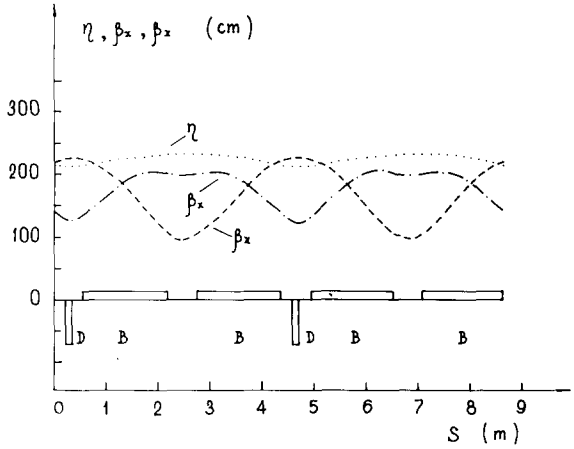

Fig. 1. Dispersion η and betatron β_x and β_z functions of the storage ring Siberia-1.

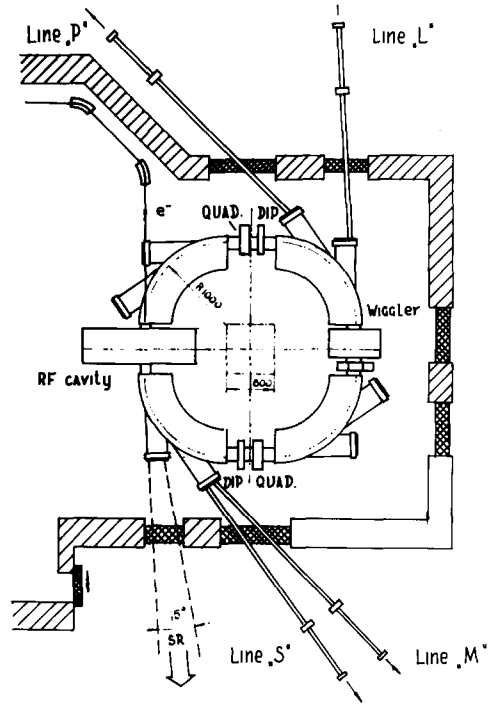

Fig. 2. Layout of the magnetic system and SR channels of the storage ring Siberia-1.

0168-9002/86/$03.50

Table 1
Basic specifications of the Siberia-1

Maximum energy, E	450 MeV (project)
	450 MeV (attained)
Beam current, I	100 mA (project)
	130 mA (attained)
Energy losses per turn, ΔW	3.63 keV
Damping times, τ_x, τ_z, τ_s	7.15, 7.15, 3.57 ms
Emittance, ε_x	8.8×10^{-5} cm·rad
Acceptances, A_z	0.56×10^{-2} cm·rad
A_x	1.4×10^{-2} cm·rad
Bunch length, $2\sigma_s$	59.9 cm
Lifetime with respect to quantum fluctuations, τ_q	6.4×10^{7} s
Beam lifetime (15% coupling, beam current 100 mA, RF-peak voltage 15 kV) τ_r	2.0×10^{4} s
Lifetime of the beam scattered on the residual gas, τ_g	3.6×10^{4} s
Rms energy spread in the beam, σ_E/E	0.39×10^{-3}
Revolution frequency, f_0	34.525 MHz
Harmonic number, k	1
RF peak voltage V_{RF}	15 kV
Energy aperture, $(\Delta E/E)_{max}$	2.9×10^{-3}
Vacuum pressure, P	10^{-9} Torr

sections 2 and 3. The cubic nonlinearity is compensated in straight section 4 by an octupole lens. Straight section 3 is also used to install the snake and a quadrupole of 5 cm length with a maximum field gradient of 20 T/m. The latter is needed to compensate for a shift in the betatron frequency, which occurs when switching the snake on.

There are the dipole coils in the quadrupole which create B_x for the correction of the vertical orbit distortions occurring with the snake field on.

2. Design of the snake

The snake comprises four main components: a superconducting magnetic system, helium volume, nitrogen volume with a heat screen and a vacuum chamber with the outer body.

The magnetic system consists of three dipoles (see Fig. 3), each having two independent poles with superconducting windings.

The core of the magnet is made of steel "armko" with a winding manufactured from a superconducting cable of Ni–Ti alloy, similar to the superconducting snake installed at the storage ring VEPP-2M [2]. Three poles (one from each magnet) are attached to a steel plate "armko" being simultaneously a magnet core. The central and the side poles are shifted by 5 mm towards the opposite directions relative to the axis of the storage

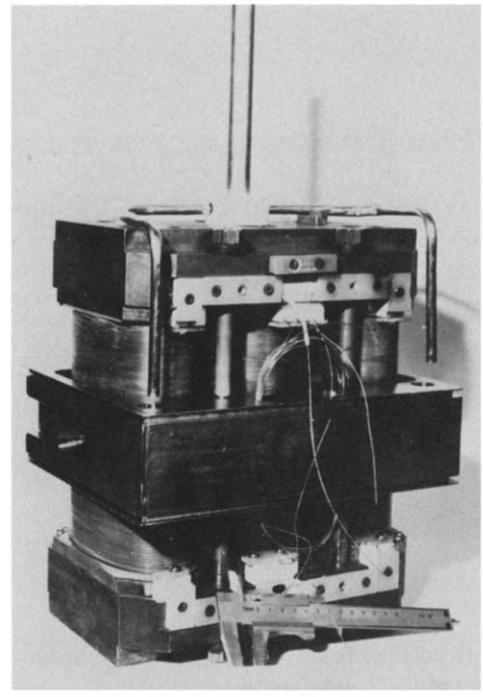

Fig. 3. Magnetic system of the 3-pole superconducting snake: 1 – plate of the magnetic core, 2 – poles of the magnets with SC windings, 3 – central plate, 4 – studs.

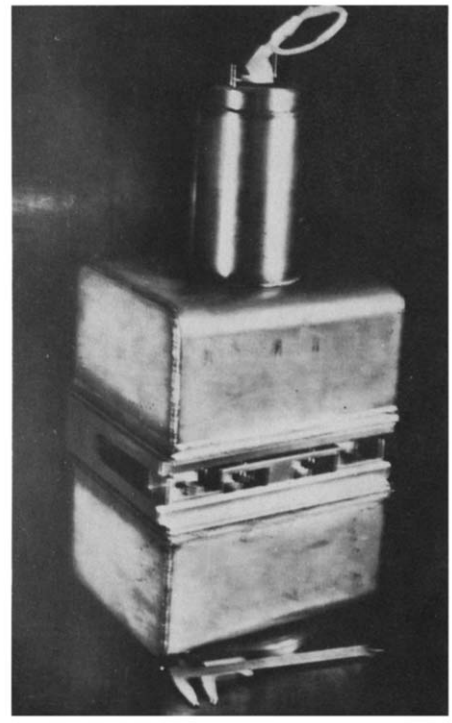

Fig. 4. Helium volume of the superconducting snake.

ring. Two plates with the poles are placed one above the other on the central stainless steel plate forming a set of three dipoles with the 32 mm interpole gap. Mounting is performed by means of four rods thereby making the construction mechanically rigid.

The magnetic system has the upper and lower caps welded to the central plate, thereby forming the helium volume (fig. 4). The central plate has a longitudinal slot allowing the helium volume to be pulled over the storage ring vacuum chamber. This makes it possible to assemble (disassemble) the snake without the deterioration of the vacuum of the storage ring.

The helium volume is located on the base plate of the nitrogen volume using three supports on the rolls made of pyrex glass with low heat conductivity.

The nitrogen volume is installed on four thermocompensating racks on the bottom of the snake body. It is connected to the upper wall of the snake body by four nitrogen lines. The nitrogen volume covers the helium volume from three sides. In turn, the latter is entirely closed by copper screens with good heat conductivity, at nitrogen temperature.

The vacuum chamber of the snake is a component of the whole vacuum chamber of the storage ring Siberia-1. The vertical aperture in the snake chamber is 22 mm, just as in the chamber of the bending magnets. In the course of operation the snake chamber is at the temperature of nitrogen.

The body of the snake provides a protection vacuum and the walls serve as a magnetic screen also. A cryostat is installed on the upper horizontal wall of the body and a vacuum magnetodischarge pump is located on the lower one by means of an adapter.

The complete snake is located on a support being simultaneously a table to assemble and disassemble the device in question on the spot. To make the disassembly easier, there is the guide, in the body, with a trolley rolling on it. On this trolley the helium volume is extended from the body together with the heat screens after the nitrogen volume and the upper cover of the body have been removed. The main specifications of the snake are given in table 2.

Table 2
Main specifications of the snake

Overall dimension (in mm)		
Length (towards the pass of the beam)		350
Width		700
Height without the cryostat		682
with the cryostat		2350
Consumption of liquid helium with the cryostat (l/h)		~ 5
Capacity of the helium volume with the cryostat (l)		110
Capacity of the nitrogen volume (l)		
of the snake		28
of the cryostat		20
Sizes of the core and superconduction winding (in mm)	Central magnet	Side magnet
Small semi-axis	25	12
Large semi-axis	45	47
Height of the SC winding	68	68
Thickness of the SC winding	22	20.5
Diameter of SC winding wire	0.85	0.85
Number of turns in the winding	1656	1518

3. Influence of the magnetic fields of the snake on the particle motion in the storage ring

3.1. Magnetic field of the snake

During the tests the magnetic field attained in the interpole gap of the central magnet is 5.8 T at a current of 264 A. Fig. 5 illustrates a diagram of the dependence of the magnetic field at the centre of the inter-pole gap of the central magnet on the current in the winding.

Fig. 6 shows the measured distribution of the vertical component $B_z(s)$ of the magnetic field along the snake axis. This distribution is well approximated by sine functions with half-periods $d_1 = 7$ cm and $d_2 = 10$ cm for the fields of the side and central magnets, respectively. The magnetic measurements have been performed under the condition $\int B_{x,z}(s)\mathrm{d}s = 0$ with a high precision for fields of different levels.

According to the calculations, the distribution of the magnetic field of the snake for the side and central poles is possible to approximate, in a horizontal direction, by the function $\cos(\pi x/a_i)$, $i = 1$ for the side and

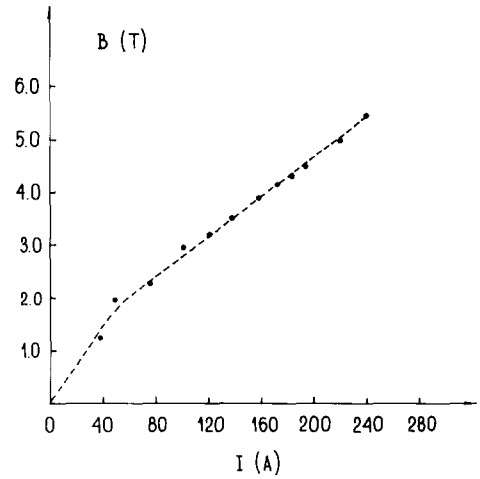

Fig. 5. Magnetic field in the gap of the central snake magnet vs the current in the winding.

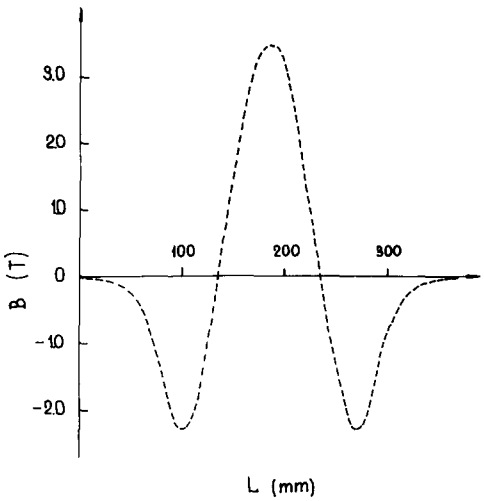

Fig. 6. Distribution of the vertical component of the magnetic field B_z along the snake axis.

$i = 2$ for the central poles. Here $a_1 \simeq a_2 = a = 14$ cm.

In a description of the particle motion in the snake one can use the expansion of the fields near the unperturbed orbit including the terms quadratic with respect to the displacement ($Z = 0$). In the general case, with the pole centres shifted in a horizontal direction from the snake axis by the quantities x_{0i}, an expression for the magnetic field on an ith section of the equilibrium orbit $x_i(s)$ is of the form

$$B_{zi} = B_{0i}\left[1 - \frac{\alpha^2(x_i(s) - x_{0i})^2}{2}\right]\sin \kappa_i s, \qquad (1)$$

where $i = 1$ corresponds to the field in the gaps of the side magnets, $i = 2$ in the gap of the central magnet, and x, z, s are the horizontal, vertical and azimuthal coordinates; $\alpha_i = \pi/a_i$ and $\kappa_i = \pi/d_i$. The sextupole term in the expansion of the field B_{zi} causes the magnetic field gradient and, hence, the focusing which depend on $x_i(s)$. An expression for this gradient is as follows:

$$G_i(x_i(s), s) = -B_{0i}\alpha_i^2[x_i(s) - x_{0i}]\sin \kappa_i s. \qquad (2)$$

The equilibrium trajectory $\kappa_i(s)$ is easy to find under the assumption that the snake field is independent of the horizontal coordinate ($x_i(s) \ll a$). At a nominal magnetic field in the gap of the central magnet $B_{02} = 4$ T ($E = 450$ MeV) the deflection of the equilibrium orbit in the snake and the amplitude of the bending angle of electrons in the snake are equal, correspondingly, to $x_{max} = 0.57$ cm and $\theta_{max} = 0.085$ rad. Note that the polarity of switching on the snake is such that the deflection is directed inwards in the ring.

3.2. Influence of the snake on the particle motion

The influence of the snake on particle motion in the storage ring is the appearance of the shifts of betatron frequencies $\Delta\nu_x$ and $\Delta\nu_z$, as well as the distortion of the equilibrium orbit and the change in the damping decrements of horizontal and longitudinal oscillations.

(a) The shifts of betatron frequencies are due to the presence of the end focusing and to the focusing caused by the collapse of the magnetic field in a horizontal direction, which is associated with the finite sizes of the poles in this direction. Provided that β_x and β_z are constants of the snake length, the resultant expressions for $\Delta\nu_x$ and $\Delta\nu_z$ may be represented as follows:

$$\begin{aligned}\Delta\nu_x &= x_1\beta_x B_{02} - x_2\beta_x B_{02}^2,\\ \Delta\nu_z &= -x_1\beta_z B_{02} + x_2\beta_z B_{02}^2 + \xi\beta_z B_{02}^2.\end{aligned} \qquad (3)$$

The whole shift $\Delta\nu_x$ and the first two terms for $\Delta\nu_z$ are due to the shift of the poles ($\Delta x = x_{01} - x_{02} \neq 0$) and to the collapse of the field ($a^{-1} \neq 0$). The third term in $\Delta\nu_z$ is due to the end focusing of the snake magnets with planeparallel edges [4]. Here

$$x_1 = \frac{1}{2}\frac{\Delta x d_2}{a^2}\frac{1}{B\rho},$$

$$x_2 = \frac{1}{2\pi}\frac{d_2^2}{a^2}\frac{(3d_1/8 + d_2/4)}{(B\rho)^2},$$

$$\xi = \frac{1}{16\pi}\frac{d_2(2 + d_2/d_1)}{(B\rho)^2}.$$

B_{02} is the amplitude of the magnetic field in the central magnet and $B\rho$ is the magnetic rigidity.

Fig. 7 shows the variation in the position of the working point on the diagram ν_x, ν_z in the process of switching on the snake. The complex trajectory of this point is accounted for by a joint action of the magnetic field of the snake and quadrupole gradients being changed. At an energy of 450 MeV, the betatron frequencies $\nu_z = 0.8492$ and $\nu_x = 0.8113$ correspond to the initial working point and at $B_{02\,max} = 4.3$ T, $\nu_z = 0.9086$ and $\nu_x = 0.8482$ at the finite working point. If we subtract the focusing associated with a variation of the gradients in the quadrupoles (whose effect on the betatron frequencies was calibrated), then we obtain the shifts in the betatron frequencies $\Delta\nu_x$ and $\Delta\nu_z$ determined only by the fields in the snake. In fig. 8 $\Delta\nu_x$ and $\Delta\nu_z$ are shown by points as the functions of a magnetic field in the gap of the central pole of the device. The possible errors made in the measurements of betatron frequencies are marked by vertical dashes. They are explained by the presence of synchrobetatron resonances, $\Delta_{x,z} = \pm\nu_s = 2.5 \times 10^{-3}$. It is seen from the diagram that $\Delta\nu_z = 0$ at $B_{02} = 3.5$ T hence the edge focusing vertical betatron tune shift is completely com-

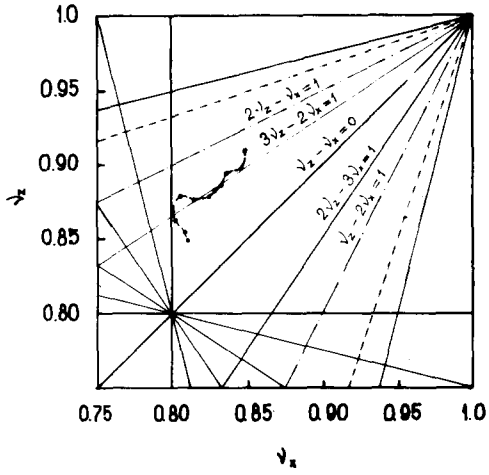

Fig. 7. Position of the working point on the diagram ν_x, ν_z in the process of switching on the snake.

pensated by the tune shift opposite in sign, arising from the shift of the poles in the horizontal direction and by the collapse of the field. The expressions (3) for $\Delta\nu_x$ and $\Delta\nu_z$ well approximate the experimental points at $a = 13$ cm, $\beta_z = 111$ cm and $\beta_x = 169$ cm.

(b) An optical system in the storage ring Siberia-1 is intended to observe the parameters of the beam [5]. The x and z coordinates of the orbit are observed simultaneously in each of four bending magnets of the storage ring. The specific feature of the operations of the storage ring with the snake is that the latter is switched on only at an energy of 450 MeV while at the injection energy $E = 60$ MeV and in the course of increasing the energy up to a maximum one the snake is switched off. For this reason, it is necessary to control the field of the remanent magnetization of the snake off at the injection energy. The measured remanent magnetization was $\int B_z \mathrm{d}s = 1.1 \times 10^{-4}$ T·m. At $\sqrt{E} = 60$ MeV this provides the orbit distortion $\delta x \leq 1$ mm.

The orbit distortions due to the incorrect compensation of the total bending angle in the snake is $\delta x = 0.5$ mm. Fig. 9 shows the experimental dependence of $\Delta I(I_1)$ of the difference in currents in the windings of the central pole I_2 and side poles I_1 on the current in the windings of the side poles; in addition, $\int B_z \mathrm{d}s \lesssim 7.5 \times 10^{-4}$ T·m ($\delta x < 0.5$ mm). We would like to emphasize the linearity of this dependence in the current range $I_1 = 20$–158 (A) which corresponds to the magnetic-field range in the central magnet gap $B_{02} = 0.65$–4.3 (T) (see fig. 5). Within the interval $I_1 = 0$–25 (A) the difference in currents $\Delta I < 0$ is negative, and the dependence $\Delta I(I_1)$ is nonlinear. Such a behaviour may be explained by the initial position of the equilibrium horizontal orbit at the moment of switching on the snake when $|x_{02}| < |x_{01}|$, i.e. when the orbit is nearer to the center of the central pole, and by the quadratic dependence of the magnetic field along the x-coordinate.

(c) When switching on the snake, the damping of horizontal betatron oscillations $J_x = 1 - D$, decreases drastically, while the damping decrement of synchrotron oscillations $J_s = 2 + D$ increases. Here

$$D = \frac{\oint \eta \left(\left| \frac{B}{B\rho} \right|^3 + 2 \frac{GB}{(B\rho)^2} \right) \mathrm{d}s}{\oint \left(\frac{B}{B\rho} \right)^2 \mathrm{d}s} . \qquad (4)$$

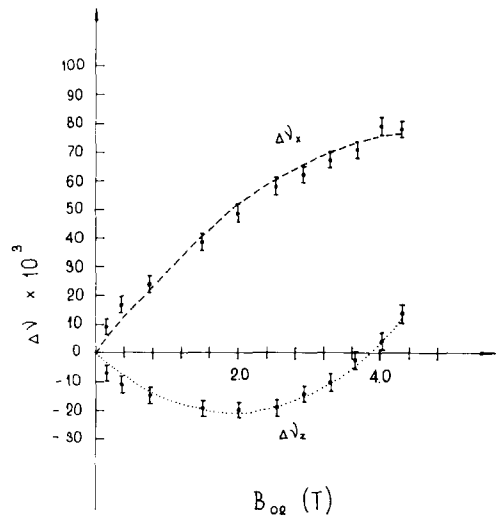

Fig. 8. Experimental shifts in betatron frequencies $\Delta\nu_x$ and $\Delta\nu_z$ vs the magnetic field in the gap of the central pole of the snake

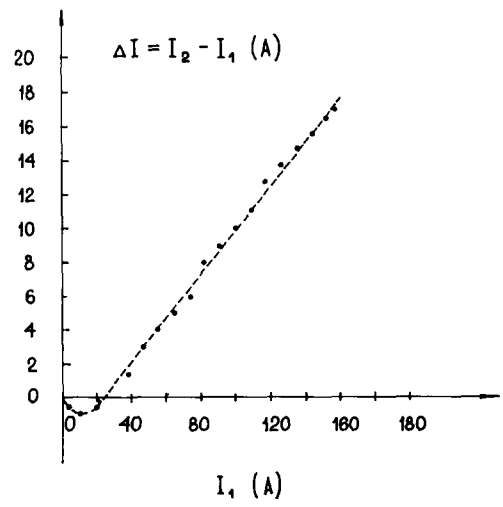

Fig. 9. Experimental dependence of the difference in currents $\Delta I = I_2 - I_1$ on the current I_1 in the side magnets of the snake; $\int B_z \mathrm{d}s < 7.5 \times 10^{-4}$ T·m and $\delta x < 0.5$ mm.

Table 3
Parameters of the SR beams at $I = 100$ mA and $E = 450$ MeV

Parameter	Magnet	Snake
Operating field	1.5 T	4.3 T
Critical wavelength	61.3 Å	21 Å
Effective length		24 cm
$K = 0.93\,\lambda_{sn}$ (cm)$\cdot B$(T)		~ 80
Angle of divergence in vertical direction $\Delta\psi_{1/2} = 1/\gamma$	0.6 mrad	0.6 mrad
Effective horizontal angle $\Delta\theta_{1/2} = 0.6\,K/\gamma$		~ 55 mrad
Flux of photons $\dot{N}$[Ph/(s·mrad·0.1% $\Delta\lambda/\lambda$)]$_{\lambda_c}$	0.7×10^{12}	0.7×10^{12}
Number of SR extraction channels	6	1
Radiated power	363 W	~ 40 W
Sizes of the electron beam at a coupling of 0.1		
$\sigma_x \times \sigma_z$	1.62×0.13 mm^2	1.9×0.1 mm^2
$\sigma_{x'} \times \sigma_{z'}$	0.65×0.08 mrad^2	0.7×0.08 mrad^2

The variation in decrements is mainly determined by the growth (with increasing the field in the snake) of the term in the expression (4) containing the integral $2\int_{sn}\eta(GB/(B\rho)^2)\mathrm{d}s$ and is connected with the collapse of the magnetic field of the snake in a horizontal direction. The separation of the poles makes this effect only stronger.

The product of the GB is the function of x_{01} and x_{02}, i.e. of the shifts of the poles relative to the unperturbed equilibrium orbit. In the case of varying the equilibrium pulse, i.e. the position of the equilibrium orbit, the magnitude of GB is varied as well. The range measured with respect to the revolution frequency f_0, with the damping in it, is $34.47 < f_0 < 34.57$ MHz, with the central frequency $f_0 = 34.5$ MHz.

4. Conclusion

The process of switching on the snake field is computer-controlled. The experimentally found relations between the currents I_1 and I_2 in the windings of the poles are kept by programming. The initial rate of inducing the current is $(\mathrm{d}I/\mathrm{d}t)_{min} = 0.15$ A/s and the maximum rate is $(\mathrm{d}I/\mathrm{d}t)_{max} = 1.5$ A/s. The system of stabilizing the power supply sources of the snake provides a maximum relative dynamical error of the currents: $\delta(I_2 - I_1)/I_1 \leq 5\times10^{-4}$. The time necessary to switch on the snake is 160 s. The field rise is performed, in practice, without the losses in electron current up to a magnetic field in the snake of 4.3 T. The SR beam from the snake with the characteristic wavelength $\lambda_c = 21$ Å is extracted into the channel in order to be utilized at the X-ray radiation. The parameters of the SR beams from the bending magnets and from the snake of Siberia-1 are listed in table 3.

In conclusion, the authors want to express their deep gratitude to the collaborators of the Kurchatov Institute (Moscow) Buzulukov Yu.P., Podogov Yu.L. and Yupinov Yu.L. and the collaborator of the Nuclear Physics Institute (Novosibirsk) Levichev E.B. for their assistance in the work of putting the snake into operation.

References

[1] V.V. Anashin et al., in: Proc. of the 7th Nat. Conf. on Charged Particle Accelerators. Dubna (1980) vol. 1, p. 306.
[2] V.V. Anashin et al., Preprint INP 84-123, Novosibirsk (1984).
[3] M. Sands, SLAC-121 (1970).
[4] L.M. Barkov et al., Preprint INP 78-13, Novosibirsk (1978).
[5] E.I. Zinin, Thesis, INP, Novosibirsk (1984).